SYSTEM PERFORMANCE ANALYSIS OF INS/DGPS INTEGRATED SYSTEM FOR MOBILE MAPPING SYSTEM (MMS)

A. W. L. Ip [a], N. El-Sheimy [a], M. M. R. Mostafa [b]
[a]Mobile Multi-Sensor Research Group
Department of Geomatics Engineering, University of Calgary,
2500 University Drive NW, Calgary, Alberta, T2N 1N4 Canada
awlip@ucalgary.ca, naser@geomatics.ucalgary.ca
[b] Applanix Corporation, 85 Leek Crest, Richmond Hill, Ontario, L4B 3B3, Canada – mmostafa@applanix.com

Commission VI, WG VI/4

KEY WORDS: Aerial Mapping, Aerotriangulation, GPS, INS, Direct Georeferencing, Boresight Calibration

ABSTRACT:

Major progress has been made in Mobile Mapping Systems (MMS) over the last few years in terms of sensor resolution, size, data rate, power requirements, and cost, besides the advances in sensor integration and data post-processing and filtering techniques. Thus, the use of such systems in different mapping applications has become cost-effective, and an enabling technology in some applications. This paper examines several topics that are critical for properly operating a mobile mapping system for different platforms and for different applications. Sensor placement, sensor synchronization, system calibration and the sensors' initial alignment are discussed in some detail. Features common to most systems will be identified and a unified model for MMS integration for airborne and land mapping application is presented where the suitable observables are assessed, and factors affecting system performance are discussed. An example from a commercial airborne MMS will be presented in some results.

1. INTRODUCTION

The parameters of exterior orientation, three translations and three rotations, essentially describe rigid-body motion in space. If a system that measures rigid-body motion can be installed on a vehicle, then the translations and rotations of the vehicle can be directly determined as time varying vectors. The process of determining these values by independent sensors is often called geo-referencing. Today, georeferencing is most easily accomplished by integrating the measurements of an inertial measuring unit (IMU) with those of GPS receivers used in differential mode (DGPS). The IMU/DGPS integration gives translation and orientation parameters for the vehicle as solutions of a system of differential equations, i.e. as functions of time.

Mobile mapping systems (MMS) consist of two major components, an imaging component and a geo-referencing component. The imaging component may be an optical or digital camera, a multi-spectral pushbroom scanner, an interferometric radar system, or a scanning laser system. If digital cameras are used as the imaging component and are fixed to the same rigid body as the IMU and the GPS antenna (i.e. to the aircraft), then the parameters of exterior orientation can simply be determined by interpolating the translation and rotation vectors at the moment of exposure. These parameters can be stamped on each digital image. In this way, the complex time-dependent positioning problem is transformed into a spatial problem from which time has been eliminated as a variable. This obviously requires very accurate time synchronization between the different sensors. The resulting geo-referenced digital images obtained in this way become the building blocks for the digital mapping program. It should be noted that a multi-sensor system defined in this way is completely self-sufficient, i.e. only data collected in the vehicle are needed to solve the georeferencing problem. It is independent of ground control because GPS, by linking into a system of Earth- orbiting satellites, will output all its results in an Earth-fixed, Earth-centered coordinate frame – the WGS 84, see Figure 1 for an example of the concept of airborne-bases MMS. MMS thus provides an integrated problem solution, rapid data acquisition, fully digital data storage, and great flexibility in post-mission data processing. Some important parameters play a role in that case such as sensor placement, sensor synchronization, system calibration, and initial alignment, which will be discussed in some details in the next few sections.

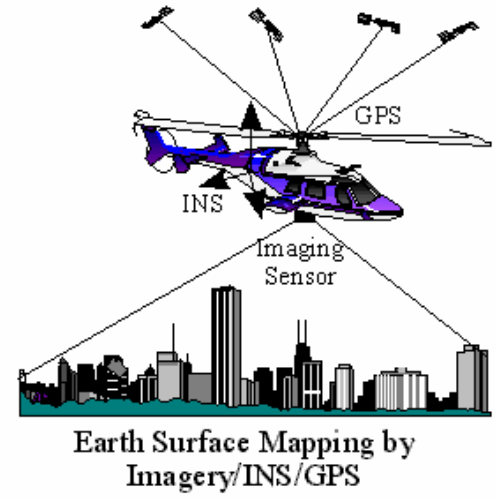

Figure 1. An Airborne MMS

2. DIRECT GEOREFERENCING USING INS/GPS INTEGRATION

The main components of a direct georeferencing system for mobile mapping use different technologies. GPS uses range measurements from satellites and INS uses gyros and accelerometers to measure angular velocity and specific force. Table 1 lists the characteristics of a stand-alone GPS, a stand-alone INS and an integrated GPS/INS.

Table 1. General difference between GPS and INS

	Advantage	Disadvantages
INS	• Self contained and independent system • Continuous data acquisition • Three positioning and three attitude components • High data sampling rate (up to 256 Hz)	• Sensor errors grow with time causing positioning error divergence
DGPS	• High accuracy of position and velocity estimation • Time-independent error model	• Losses of lock causing gaps in positioning • Low data sampling rate (1-10 Hz) • Slow ambiguity resolution time over long baseline and/or in presence of higher ambient noise
INS / DGPS	• Combine all advantages of both systems • Redundant and complementary data (both systems' errors are separately observable) • Navigation through GPS outages • GPS fixes allow INS error estimation	• No significant limitations • Precise time synchronization needed

As depicted in Table 1, the low noise and high bias INS and the higher noise and low bias GPS are complementary systems. Their integration, therefore, reduces or eliminates their limitations.

2.1 The Unified Georeferencing Model

Direct georeferencing mathematical model has been used for numerous applications in land, airborne and marine applications (c.f., Schwarz, el al, 1993, El-Sheimy, 1996a, Mostafa, 2003). Several forms of the mathematical model have been previously presented to accommodate a certain application. In this Section, the basic unified formula is re-visited. As shown in Figure 2, the georeferencing basic model can be expressed by:

$$r_p^m = r_{INS}^m(t) + R_b^m(t)(sR_c^b r^c - a_1^b) \quad (1)$$

where, $r_{INS}^m(t) = r_{GPS}^m(t) - R_b^m(t)a_2^b$ (2)

therefore $r_p^m = r_{GPS}^m(t) + R_b^m(t)(sR_c^b r^c - a_1^b - a_2^b)$ (3)

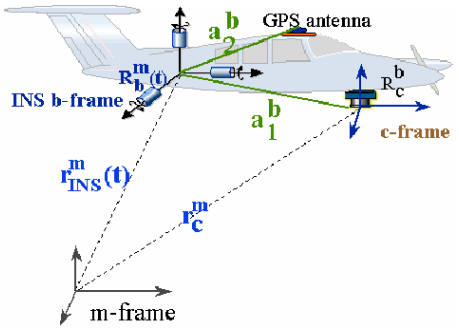

Figure 2 The Direct Georeferencing Model

The different terms in Equations 1, 2, and 3 are explained in Table 2.

Table 2. Terms of georeferencing equation

Variable	Description
r_p^m	Position of the point of interest represented in mapping frame
$r_{GPS}^m(t)$	GPS antenna position represented in mapping frame
$R_b^m(t)$	Rotation matrix between INS body frame and mapping frame
s	Scale factor between camera image space and object space
R_c^b	Rotation matrix between camera frame and body frame
r_c	Location of the point of interest represented in camera frame
a_1^b	Lever arm offset between INS body frame and camera frame
a_2^b	Lever arm offset between INS body frame and GPS antenna

For a MMS system, a number of parameters play a role when the system performance, accuracy, and reliability are concerned. These parameters can be summarized as:

1. Sensor placement – It is imperative that relative sensor placement in the carrier platform be taken into account. This includes the different sensor position and orientation offsets as previously presented in Table 2 by the lever arms and the rotation matrix between the camera frame and the INS body frame
2. Synchronization – the synchronization is the process by which the different sensors in a MMS are relatively brought to one unique time frame.
3. Calibration – the calibration is the process by which the relative positions and orientation of each sensor with respect to a reference frame is established. Once calibration is done, all different streams of sensor data can be properly fused.
4. Initial alignment – all sensor generates errors, it must be minimized before mapping mission starts.

Next, the aforementioned issues will be discussed in some detail.

2.2 Sensor Placement

For a mobile mapping system used in land or airborne, GPS, IMU, and an imaging sensor tend to be the common sensors to be used efficiently. In some other instances, such as in a land-based application, some dead reckoning systems might be integrated with the three main sensors to help improve the overall performance in case of GPS signal blockage in urban canyons. However, this paper will only focus on the integration of the first three sensors. The inter-relationship between these primary sensors is defined by lever arms and mis-alignment angles; these calibration terms are discussed in the following:

Imaging Sensor Installation

This sensor usually has a fixed location because it normally is located where the scene of interest is visible for image acquisition. Therefore, imaging sensor is placed on the front roof of the vehicle in land applications, and is placed at the bottom of the aerial photography aircraft in airborne applications.

GPS Antenna Installation

The GPS antenna has to be always visible to all satellite antennas for proper GPS signal reception at all times. Therefore, the GPS antenna is placed outside of the platform for proper signal reception. In land applications, it can be placed anywhere on the rooftop of the vehicle. But for calibration efficiency, it is usually mounted as closely as possible to the imaging sensor. In airborne applications, the same concept applies. It is preferable to even mount the GPS antenna directly above the centre of the imaging sensor lens. In addition, the aircraft wings are also taken into consideration, in order to prevent GPS blockage during large banking angles. Practically, pilots will have to take wider turns to minimize banking angles. Thus, the location of the GPS antenna is more flexible and can be located as closely as possible to the INS sensor.

IMU Installation

An IMU is a self contained instrument and does not have a specific installation requirement except for rigidly mounting it to the imaging sensor. Rigid mounting the IMU is a key factor in all mobile mapping systems because of the assumption made in the georeferencing formulae which is the constant rotation matrix between the IMU body frame and the camera frame. It, therefore, established a critical calibration parameter called boresight (the angular misalignment between the IMU and camera frames). Boresight calibration is done at system installation and periodically as a quality control of the entire mobile mapping system, for details on boresight calibration see Mostafa, 2001 for airborne applications and El-Sheimy, 1996b. Figure 3 shows an airborne example of IMU mount on the camera head in the Applanix DSS, while Figure 4 shows the entire system installation onboard an aircraft. A number of other airborne digital systems has been designed to rigidly install the IMU directly on the camera head such as the Leica ADS40 and the Z/I Imaging DMC cameras. In land-based applications, multiple imaging sensors are normally used for coverage purposes. Therefore, the INS is rigidly mounted on a platform that holds all imaging sensors together, to allow for constant boresight matrix at all times. Figures 5 and 6 shows sensor installation onboard The VISAT of The University of Calgary.

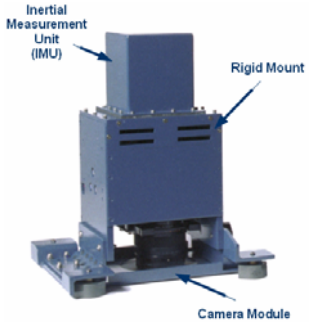

Figure 3. Rigid Mount for Camera/IMU of the DSS

Figure 4. DSS Aircraft Installation

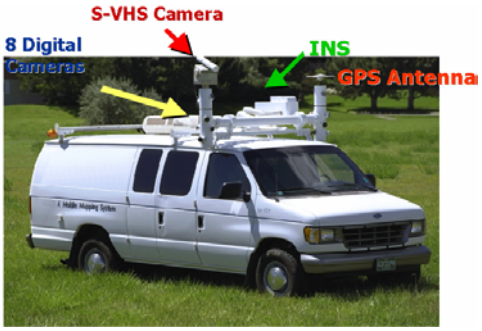

Figure 5. VISAT of The University of Calgary

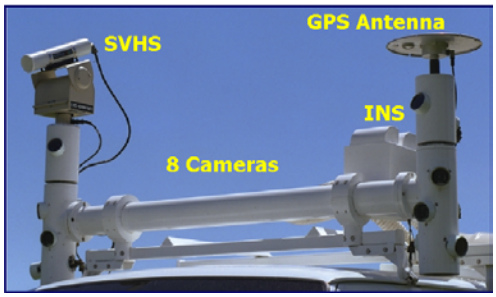

Figure 6. Sensor Installation onboard of the VISAT

2.3 Synchronization

For high accuracy position and orientation determination by MMS, precise synchronization is very important. The three

sensors: GPS, INS and imaging sensor operate at their own time frame. In addition, data logging is typically done using computer components that have their own frequency oscillators. The synchronization of all different components is an essential assumption in the direct georeferencing case. In principle, GPS provides the best time reference with GPS time. INS comes with an integrated timing module, but is rarely directly synchronized with GPS On the other hand, imaging sensors do not come with any timing module, and the acquisition of imagery does not occur at a fixed time interval. Resolving this timing problem, newer imaging sensors provide a linkage to the GPS receiver, in order to time-tag the imagery exposure time.

Whether it is real-time or post-processing integration, interpolation will be used to synchronize all the measurements from the different sensors. Since all measurements are collected by the controlling computer system with physical connections, data transmission delays must be considered. Such delays can result from cable length, computer clock error or A/D conversion. For precise system design, these delays can be determined easily and calibrated from synchronization.

Synchronization error (δt) introduces both position and attitude error. Position error is a function of velocity and attitude error is a function of angular velocity. Therefore, synchronization error is directly proportional to application dynamics. The combined error presented in direct georeferencing can be formulated by modifying Equation 3 to replace the GPS antenna position with a platform velocity v(t) and to replace the rotation matrix between INS body and mapping frames with an angular velocity vector w(t). This results in:

$$\delta \dot{r}_p^m = \delta t[v(t) + w(t)(sR_c^b r^c - a_1^b - a_2^b) \qquad (4)$$

For demonstration purposes, a simulation has been done using a DSS flight with an average speed of 180 km/h. Figure 7 presents the flight trajectory and the dynamics of the aircraft during image acquisition on two flight lines over a span of 15 minutes. A 1 millisecond of synchronization error has been introduced. The corresponding position and attitude errors are shown in Figure 8 and the statistic report is listed in Table 3.

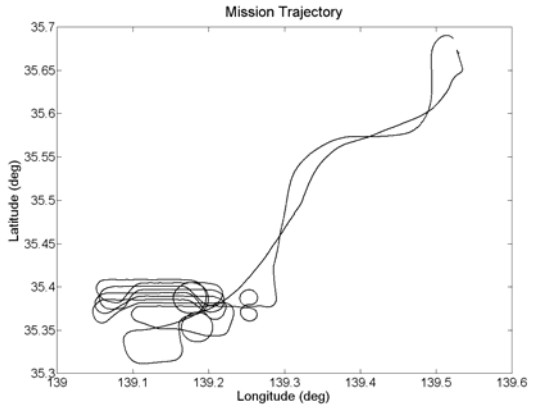

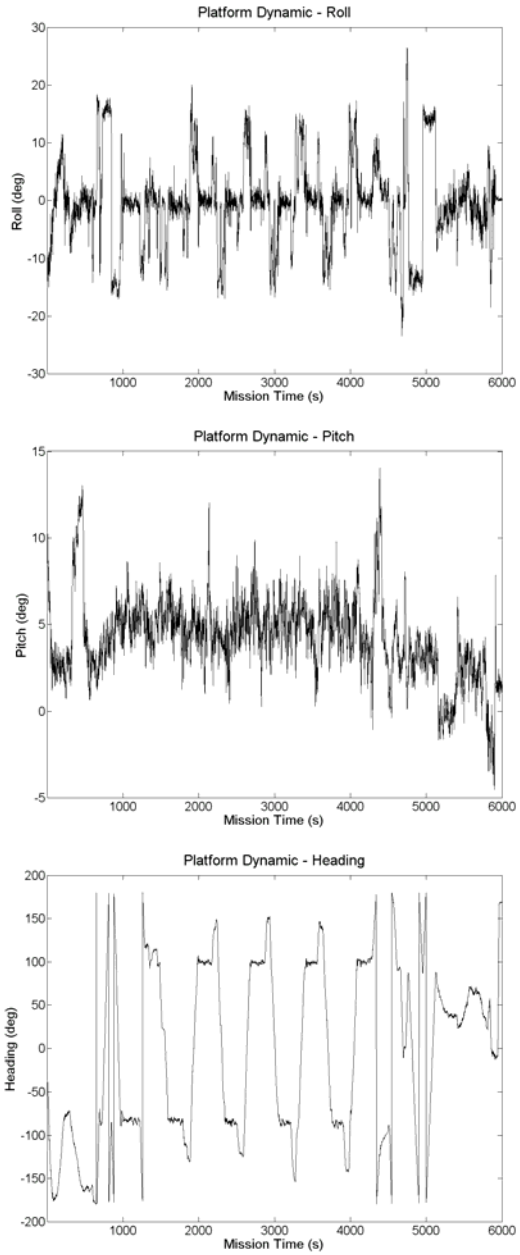

Figure 7. DSS Flight Trajectory and dynamics during image acquisition

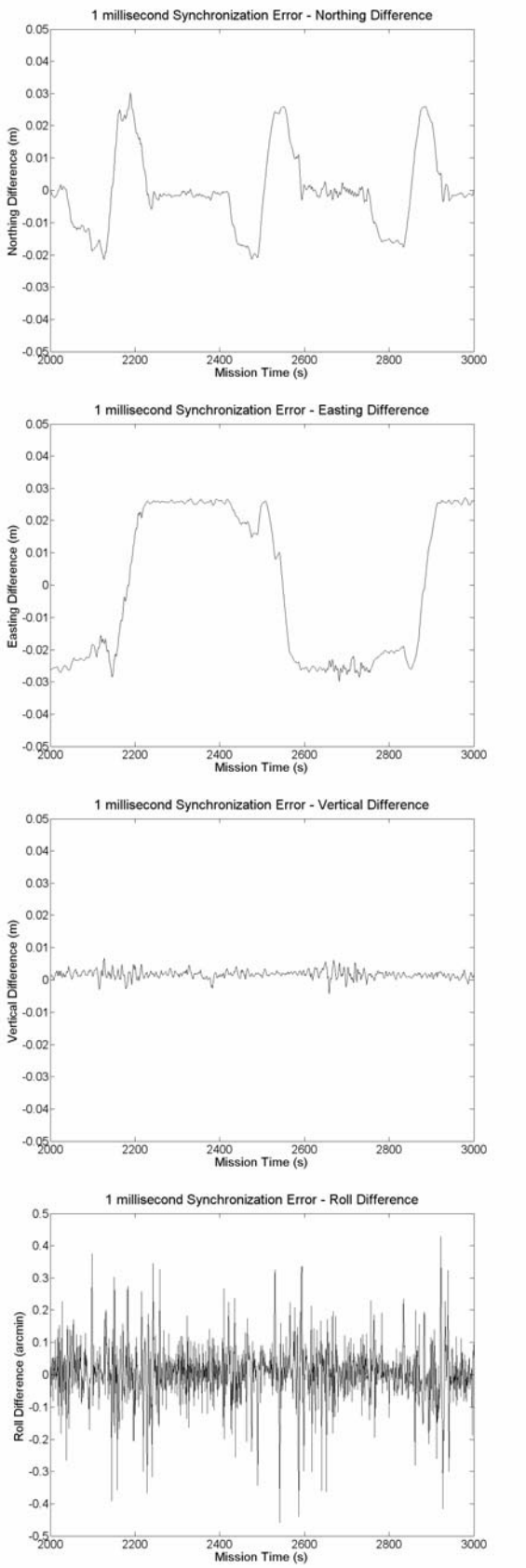

Figure 8. Navigation error due to 1 ms synchronization error

Table 3. Statistics of Synchronization Error Influence on Navigation Position and Attitude in Post-Processing, 1 millisecond simulation

Navigation error	Min	Max	Mean	RMS
Northing (m)	**-0.021**	**0.031**	0.000	0.012
Easting (m)	**-0.030**	**0.027**	0.000	0.023
Vertical (m)	-0.004	0.007	0.002	0.002
Roll (amin)	-0.840	0.700	0.000	0.140
Pitch (amin)	-0.280	0.320	0.020	0.060
Heading (amin)	-0.390	0.340	-0.020	0.110

Notice that Table 3 reflects the absolute value of the simulation results. Although the original data was available at 200Hz data rate, Figure 8 was plotted using a 1Hz data rate.. This down-sampling method has been applied to all figures in this paper.

1 millisecond is chosen to be used in the simulation because it is a small quantity when compared to a typical 1 MHz of the data logging computer. This value is far less than the actual IMU data rate reported (typically 200Hz). Although the statistics shown in Figure 8 and Table 3 are insignificant, these only reflect a simulation where synchronization error is small in the system. Due to the nature of electronic systems, some CCDs require up to several seconds for a single image acquisition; in this case synchronization error is relatively large. In addition, these errors will be projected to the ground which is directly related to system dynamic and project scale. Therefore synchronization error is very important especially in large scale project and missions with high dynamics. For example, in

Applanix DSS, there is a known delay (through calibration) in the CCD chip of about 2 milliseconds. When this delay is inserted in Equation 4 with the same simulation data, a 2 millisecond synchronization error should introduce twice of the error as in the 1 millisecond simulation. The result of the 2 milliseconds simulation is presented in Table 4.

Table 4. Statistics of Synchronization Error Influence on Navigation Position and Attitude in Post-Processing, 2 milliseconds simulation

Navigation error	Min	Max	Mean	RMS
Northing (m)	**-0.043**	**0.058**	0.000	0.025
Easting (m)	**-0.060**	**0.056**	0.000	0.047
Vertical (m)	-0.006	0.012	0.004	0.004
Roll (amin)	-1.690	1.400	0.000	0.280
Pitch (amin)	-0.510	0.610	0.050	0.120
Heading (amin)	-0.740	0.630	0.000	0.200

From Table 4, expected results are achieved with twice of navigation error experienced under 2 milliseconds synchronization error. As notice from both Table 3 and 4, mean values in navigation error is close to zero. This is a result of opposite flight lines where the errors are cancelled by each other. This proves that synchronization error is flight direction related and it helps to capture synchronization error in flight environment. In existence of synchronization error, change of sign will appear in difference of navigation solution on each opposite flight lines. However, when project is flown in the same direction on each flight line, synchronization can not be captured directly as it is correlated with datum shift. Therefore, calibration of synchronization error is usually carried in lab environments where static mode can be achieved. Using accurate timing equipments, synchronization error can be captured in static mode without influence from system dynamics.

2.4 System Calibration

A mobile mapping multi-sensor system calibration is critical for a successful image georeferencing. Overall system calibration is kept in mind when choosing the system installation. Equation 3 shows that there are several parameters which must be determined through calibration. There are a total of three calibration parameters, namely: Lever arm offset, Boresight misalignment, and Camera calibration. In the following subsections, these items are discussed in some detail.

2.4.1 Lever Arm Calibration:

The Lever arm describes the spatial vector difference between two coordinate frame origins of two sensors. For the case at hand, three lever arms exist between the GPS, IMU and the imaging system. However, the direct georeferencing equation deals with sensor positions and attitude angles projected from the INS body frame onto the mapping frame. Therefore, it comes down to calibrating the lever arm between the GPS antenna the IMU centre and the lever arm between the imaging system coordinate frame origin and the IMU centre.

Lever arm calibration is done using either of the following approaches:

1. Measuring the lever arms using land-survey techniques. The ease and simplicity of such an approach makes it a common process in airborne and land applications. In the airborne case, however, it's preferred to mount the GPS antenna directly above the lens centre of the imaging sensor in use.
2. Indirectly computing the lever arms using photogrammetric bundle adjustment. This way, the lever arms are modelled as unknown parameters. It, however, increases the complexity of the bundle adjustment algorithm and might introduce correlation with the GPS-derived antenna position. Therefore, such an approach is not entirely favourable from the photogrammetric stand point.
3. Indirectly computing the lever arms using the GPS and IMU measurements during data collection. Kalman filter is used for that purpose in either real-time or more accurately in post-mission. Figure 9 shows the lever arm between GPS antenna and INS, which is shown to be settled to a constant value after about 15 minutes of data collection. In this experiment, initial lever arm values for all axes are set to zero to illustrate the efficiency of Kalman Filtering. Since the resolved value of lever arm in z axis is quite away from initial value, it takes more time to converge. In actual application, initial values of lever arms are roughly determined (by tape measurements) and provided to data post-processing softcopy. Note that this method is only valid for the estimation of the lever arm between the GPS antenna and the IMU center. The lever arm between the imaging sensor and the IMU center or GPS antenna cannot be computed. In land application, this is not a problem since it can be determined using a total station. In aerial application, where the IMU is normally installed closely to the imaging sensor, the lever arm is typically measured and provided by the manufacturer.

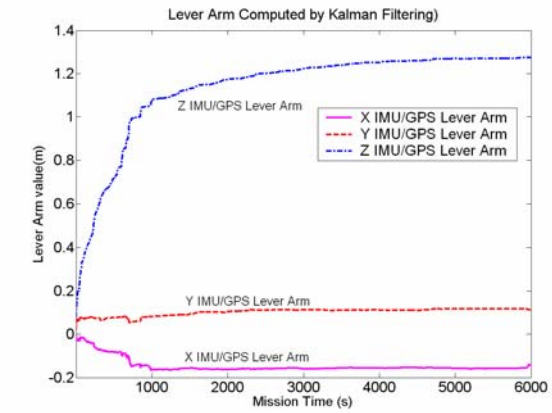

Figure 9. Lever Arm Computed by Kalman Filtering

Although a lever arm between different sensor components in a mobile mapping system is constant vector. Therefore, by intuition, any error in lever arm causes a constant bias of the image position. However, such a constant bias is projected onto the mapping frame by the time dependent rotation matrix between INS body and mapping frames, $R^m_b(t)$. Therefore, the lever arm error is also time dependent with respect to the mapping frame. It is, therefore, affected by the dynamics of the MMS platform. The lever arm error can be expressed by:

$$\delta r^m_p = R^m_b(t)(\delta a^b_1 - \delta a^b_2) \quad (5)$$

For demonstration purposes, a simulation has been done using the same DSS flight shown in Figure 7. An error of 10 cm is introduced to the x-axis lever arm (which points in the flight direction). The resulting imaging sensor position error is shown in Figure 10 and the statistic report is presented in Table 5.

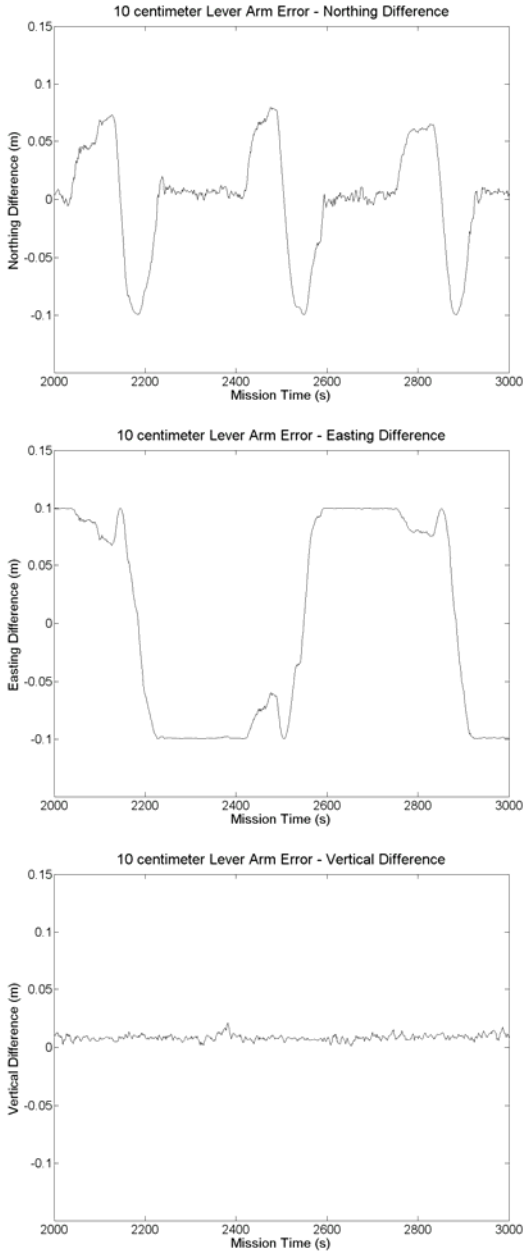

Figure 10. Position error due to 10 centimeter Lever Arm Error in flight direction

Table 5. Statistics of Lever Arm Error Influence on Navigation Position in Post-Processing, 10 centimeter simulation

Navigation error	Min	Max	Mean	RMS
Northing (m)	**-0.110**	**0.078**	0.001	0.046
Easting (m)	**-0.100**	**0.100**	0.003	0.009
Vertical (m)	0.000	0.002	0.008	0.009

The reason for choosing the 10 cm lever arm error in the simulation is because this is an average value in the DSS system. Although lever arm can have a value of sub-meter level, especially in z axis, this simulated result can provide relative influence of lever arm error. From Figure 10, lever arm error is only projected to Northing component during aircraft banking, and the rest of lever arm error is introduced to Easting component when the flight direction is parallel to x-axis. Therefore, lever arm error can be projected in both Easting and Northing components depending on the dynamics of the flight. Similar to synchronization error, lever arm error is flight direction related and there it can be captured through opposite flight lines. Further, aircraft pitching occasionally in this DSS flight, the vertical position component has also been influenced but with insignificant magnitude. Since lever arm error is a constant vector, this error is independent when determining attitude information of the platform. Therefore, no attitude error is being introduced in this simulation.

2.4.2 Boresight Calibration:

Although most care is typically done to install the IMU in perfect alignment with the imaging sensor. A residual mis-alignment angle between the two frames will take place. This is called boresight as shown in Figure 11.

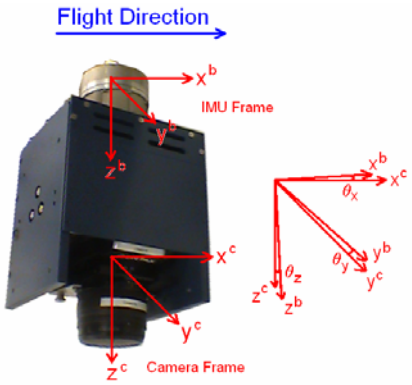

Figure 11. Camera/IMU Boresight

There are two methods to calibrate the boresight, namely:

1. Comparing the GPS/INS-derived angles with those independently computed using Aerial Triangulation (c.f., Skaloud, 1999). The constant difference between the two sets of angles is extracted as the three components of the boresight angles.
2. Computing the boresight angles as additional unknown parameters in GPS/INS-assisted Bundle Adjustment (c.f., Mostafa, 2001).

When comparing the two methods, the first method is more costly, and requires a lot more effort than the second method. On the other hand, the second method allows a ground control point – free solution. Geometrically, the second method is more

stable and therefore, camera self-calibration parameters are decorrelated easily and thus camera calibration is feasible simultaneously with the boresight calibration.

Since the IMU and the imaging sensor are typically installed in a rigid mount, boresight is assumed constant over time. This is a key assumption in the direct georeferencing technique. However, boresight angular errors are projected onto the mapping frame. Therefore, it depends on the MMS platform dynamics and is also amplified by the scale of the project; which is directly related to the flying height (h). The boresight error can be expressed by Equation 6 and an illustration of the error is shown in Figure 12.

$$\delta r_p^m = R_b^m(t)(s\delta R_c^b r^c) \quad (6)$$

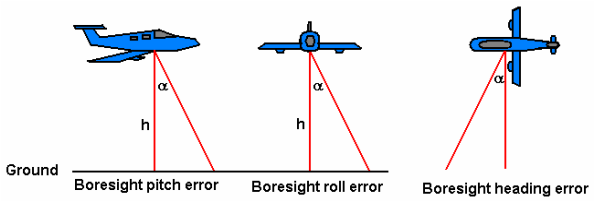

Figure 12. Illustration of Boresight Errors in Airborne Applications

For demonstration purposes, a simulation has been done using a DSS flight with a photo scale of 1:22000. A 10 arc-min boresight error is introduced on each INS axis independently. This value is chosen based on the typical boresight angle found on a DSS system. Specification of a DSS is summarized in Table 6.

Table 6. Specification of DSS

Array size	4092 X 4077 pixels, 9 micron pixel size
Lenses	Standard: 55mm – Color & CIR Optional: 35mm – Color only
Shutter Speed	1/125 – 1/4000 sec
Max Exposure Rate	2.5 or 4 sec
GSD	0.05 to 1 meter (platform dependent)
Smear	< 10% typical
Housing	Ruggedized exoskeleton with lens stabilization
Positioning accuracy	0.05 – 0.3 meter, post mission
Navigation error	0.008 – 0.015 deg, post mission
FMS	TrackAir EZtrack or external third-party
Northing (cm)	80 GB removable hard drive and pressurized data brick

The resulting exterior orientation parameters are then used to perform space intersections for 7 ground control points within the project area shown in Figure 13. Table 7 lists the RMS of the checkpoint residuals computed as the difference between the check point coordinates computed by space intersection and their values measured by land surveying techniques. The first entry of the table which is labelled "no error" shows the RMS of check point residuals of the 7 points without any intentional boresight error. The second entry labelled "x-axis" shows the RMS when an error in the boresight x-component is introduced to be 10 arc minutes. Note that the Northing component has increased by about twenty times due to the intentional simulated boresight error. Similarly, the introduction of a boresight error of 10 arc minutes on the y-component of the boresight results in increasing the Easting error by about 16 times and increasing the error in the vertical component by twice as much. This is due to the fact that the intentional boresight error is projected on the mapping frame and it affected all coordinate components. In the third entry, labelled "z-axis", an intentional boresight error of 10 arc minutes has been introduced to the z-component of the boresight angle and it resulted in degrading the Easting and Northing components by 2-3 times.

Table 7. Statistics of Boresight Error Influence on GCP Coordinate Computational Accuracy by Direct Georeferencing

Boresight error on	GCP RMS		
	Easting (m)	Northing (m)	Vertical (m)
no error	0.153	0.145	0.656
x-axis	0.141	**2.890**	0.740
y-axis	**2.455**	0.192	**1.202**
z-axis	0.494	0.401	0.762

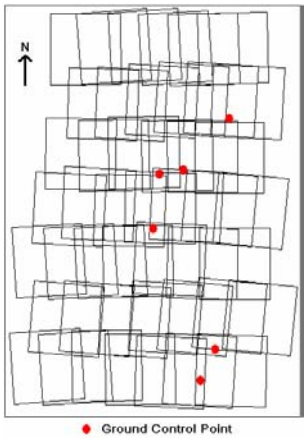

Figure 13. Block Configuration of the DSS 1: 22000 Flight

Note that, since the boresight error influence is photo scale-dependent, it is more severe in the case of airborne applications than that of the land-based applications.

2.4.3 Camera Calibration

Camera calibration is the process of determining the internal geometric and optical characteristics of the camera. This is also referred as the interior orientation of a camera system.

Interior orientation includes focal length, of principal point location, and lens distortion. Metric camera is calibrated in

laboratory periodically through certified agencies to ensure stable geometry. Except for the airborne commercial digital cameras, current cameras are not designed for photogrammetric operation and therefore the internal geometry is normally unknown. This is typical in the case of land-based applications and some airborne applications, where the user develops their own camera. In order to provide cost effective procedure for frequent self-calibration, camera calibration is normally done together with boresight calibration through a quality control of the overall system.

2.4.4 Initial Alignment

Alignment is the process of estimating the attitude information of the IMU, i.e. the direction cosine matrix (R_b^m) of the IMU with respect to the mapping frame. Static alignment is accomplished by two steps; levelling and gyro-compassing. Levelling refers to obtaining the roll and pitch of the IMU using the accelerometer outputs and gyro-compassing refers to obtaining the heading information using the gyroscope outputs. The attitude information (roll, pitch and heading) are referenced to the navigation or local-level frame (l-frame), which is an arbitrary frame and is not compatible with the mapping frame. Therefore, the alignment angles resolved through accelerometer output and gyro-compassing is instead represented by R_b^l which is the rotation matrix between the body frame and the l-frame. In order to align the IMU with respect to the mapping frame, a transformation (R_l^m) must be applied (from roll, pitch and heading to omega, phi and kappa, respectively). R_l^m defines the relationship between the two frames and therefore R_b^m can be determined from Equation 7. The resulting part is the attitude information of the IMU (R_b^m) in mapping frame with its components are as described in Equation 8.

$$R_b^m = R_l^m R_b^l \tag{7}$$

$$R_b^m = R_3(\kappa)R_2(\rho)R_1(\omega) \tag{8}$$

$$R_b^m = \begin{pmatrix} \cos\rho\cos\kappa & -\cos\omega\sin\kappa+\sin\omega\sin\rho\cos\kappa & \sin\omega\sin\kappa+\cos\omega\sin\rho\cos\kappa \\ \cos\rho\sin\kappa & \cos\omega\cos\kappa+\sin\omega\sin\rho\sin\kappa & -\sin\omega\cos\kappa+\cos\omega\sin\rho\sin\kappa \\ -\sin\rho & \sin\omega\cos r & \cos\omega\cos\rho \end{pmatrix}$$

Note that the time component (t) of $R^m{}_b(t)$ is neglected as the initial alignment process is performed in static mode. R_3, R_2 and R_1 correspond to the rotation along the axes: z (kappa), y (phi) and x (omega), respectively. Due to the angler random walk of the inertial gyroscopes, initial alignment accuracy is dependent on alignment time, especially on the Kappa angle (κ). Equation 9 expresses the relationship between alignment error in Kappa angle ($\delta\kappa$) with Angular Random Walk (ARW) in the z-gyro, the alignment time (T_a), the latitude (ϕ) at location of initial alignment and the earth rotation (ω_e). Error in initial alignment is treated as attitude error throughout the mission, and the error model is expressed in Equation 10. Since attitude errors will be amplified by the altitude of aircraft, their behaviour is similar to the boresight errors (shown in Figure 12). Note in Equation 9, Kappa accuracy is indirectly proportional to the square root of alignment time. Therefore, to achieve better Kappa accuracy, longer the alignment is required (typically 15 to 20 minutes).

$$\delta\kappa = \frac{ARW}{\omega_e \cos\phi\sqrt{T_a}} \tag{9}$$

$$\delta r_p^m = \delta R_b^m(t)(sR_c^b r^c) \tag{10}$$

After initial alignment, $R_b^l(t)$ will be updated/integrated through angular velocity measurements of the gyros. Each time $R_b^l(t)$ is updated, $R_l^m(t)$ must be applied to determine the corresponding $R_b^m(t)$, and the attitude information can be extracted through the recursive form in Equation 11.

$$R_b^m(t) = \begin{pmatrix} r_{11} & r_{12} & r_{13} \\ r_{21} & r_{22} & r_{23} \\ r_{31} & r_{32} & r_{33} \end{pmatrix}$$

and

$$\begin{aligned} \omega &= \tan^{-1}(r_{32}/r_{33}) \\ \rho &= \tan^{-1}(r_{31}/\sqrt{r_{11}^{\ 2}+r_{22}^{\ 2}}) \\ \kappa &= \tan^{-1}(r_{21}/r_{11}) \end{aligned} \tag{11}$$

Since the above attitude information is referenced to the IMU center with respect to the mapping frame; for the interest of mapping application, attitude information in the EO parameters must be referenced to the center of the imaging sensor. Therefore, boresight angle and lever arm between the imaging sensor and the IMU center must be considered and applied to complete the Direct Georeferencing equation as presented in Equation 3.

3. CONCLUSION

Direct Georeferencing is an effective tool for mapping application through multi-sensor integration. Due to the different definition of these sensors, integration parameters of these sensors must be considered and well calibrated. Certain parameters include sensor placement and synchronization, system calibration and initial alignment. For both airborne and land application, the basics behind the integration method is similar, in which the integration of three primary sensors are considered: GPS, INS and Imaging sensor. However, the operating environment controls how these sensors are related to each other, especially in the sensor placement. Therefore, the weights of calibration parameters for these two applications are different from each other, resulting different design of Kalman Filtering for implementation. Throughout the examples from the paper, it has shown that system synchronization and calibration are the most important factors to be considered. Error in system synchronization will be magnified through MMS dynamics in the Direct Georeferencing equation. However, this error is still relatively small comparing to system calibration error; also, it can be captured and calibrated through

lab environment. In system calibration, lever arm is important with its magnitude (up to sub-meter level). Error in lever arm can be projected to any position vector depending on platform dynamics. With the help of sensor specification, lever arm can be determined through installation. In addition, with the help of Kalman Filtering, lever arm with uncertainty can be calibrated throughout the mission. In boresight calibration, it is an important part on using a Direct Georeferencing system. Being an attitude error, boresight mis-alignment decreases the accuracy of EO parameters and introduces magnified ground error through operating height. Therefore, this parameter must be well-calibrated and monitor constantly through proper quality analysis/control procedures. Finally, initial alignment under static mode is important to provide accurate DGPS/INS data through out the mission. Although aligning during dynamic motion is possible with Kalman Filtering, longer epochs are required for alignment process; this lengthens mission time and is not cost efficient. Therefore, MMS is a complex system which requires knowledge on each parameters, each of them must be well calibrated/controlled to provide accurate EO parameters for direct georeferencing in either airborne or land application.

4. ACKNOWLEDGEMENTS

The authors would like to thank the financial support by NSERC and Applanix for supporting this research work.

5. REFERENCES

Ellum, C.M., N., El-Sheimy, 2002. The Calibration of Image-Based Mobile Mapping Systems. Department of Geomatics Engineering, University of Calgary, Calgary, Canada.

Ellum, C.M., N., El-Sheimy, 2001. Land-Based Integrated Systems for Mapping and GIS application. Department of Geomatics Engineering, University of Calgary, Canada.

El-Sheimy N., 1996a. A Mobile Multi-Sensor System For GIS Applications In Urban Centers. The International Society for Photogrammetry and Remote Sensing (ISPRS) 1996, Commission II, Working Group 1, Vol. XXXI, Part B2, pp. 95-100, Vienna, Austria, July 9-19.

El-Sheimy, N., 1996b. The Development of VISAT-A Mobile Survey System for GIS Applications, UCGE Report #20101, Department of Geomatics Engineering, The University of Calgary, Canada.

Grejner-Brezezinska, D.A., 2001. Direct Sensor Orientation in Airborne and Land-based Mapping Application. Report No. 461, Geodetic GeoInformation Science, Department of Civil and Environmental Engineering and Geodetic Science, The Ohio State University, Ohio, United States.

Lithopoulos, E., D.B., Reid, B., Scherzinger, 1996. The Position and Orientation System (POS) for Survey Applications, International Archieves of Photogrammetry and Remote Sensing, ISPRS Comm. III, Vol. XXXI, Part B3, pp. 467-471.

Mostafa, M.M.R., 2003. Design and Performance of the DSS. Proceedings, 49th Photogrammetric Week, Stuttgart, Germany, September 1-5, 2003.

Mostafa, M.M.R., 2001. Digital Multi-Sensor Systems – Calibration and Performance Analysis. OEEPE Workshop, Integrated Sensor Orientation, Hannover, Germany, Sept 17 – 18, 2001.

Reid, D.B., E., Lithopoulos, J., Hutton, 1998. Position and Orientation System for Direct Georeferencing (POS/DG), ION 54th Annual Meeting, Denver, Colorado, June 1-3, pp. 445-449.

Skaloud, J., 1999. Problems in Direct-Georeferencing by INS/DGPS in the Airborne Environment. ISPRS Commission III, WG III/1 Barcelona, Spain, November 25-26.

Skaloud, J., D., Cosandier, K.P., Schwarz, M.A., Chapman, 1994. GPS/INS Orientation Accuracy Derived From A Medium Scale Photogrammetry Test, International Symposium on Kinematic Systems in Geodesy, Geomatics and Navigation – KIS94, Banff, Alberta, Canada, August 30-September 2, pp. 341-348.

Skaloud, J., M. Cramer, K.P., Schwarz, 1996. Exterior Orientation by Direct Measurement of Camera Position and Attitude, International Archieves of Photogrammetry and Remote Sensing, Vol. XXXI, Part B3, pp. 125-130.

Schwarz, K.P., M.A., Chapman, M.E., Cannon, and P., Gong, 1993. An Integrated INS/GPS Approach to The Georeferencing of Remotely Sensed Data, PE&RS, 59(11): 1167-1674.